

PAPER REF: 3969

CRASH ENERGY ABSORPTION OF ALUMINIUM FOAMS WITH MODIFIED CELLULAR STRUCTURES

Nuno Peixinho^{1(*)}, Paulo Pinto¹, Filipe Silva¹, Delfim Soares¹

¹CT2M – Center for Materials and Mechanical Technologies, Universidade do Minho, Guimarães, Portugal

(*)Email: peixinho@dem.uminho.pt

ABSTRACT

This study presents experimental results on the behavior of aluminium alloy metal foams in compression. Two types of metal foams were analyzed, with uniform cell structure and with a dual-size cell arrangement seeking optimized mechanical properties. The structures were manufactured by lost-wax casting using 3D printed components for internal structure definition. Results for stiffness and energy absorption were obtained and compared on weight efficiency basis. The results are indicative of higher efficiency of the dual-size structures that may be considered for use in components subjected to impact or compression loading.

Keywords: metal foam; aluminium; energy absorption

INTRODUCTION

Following requirements of weight efficiency and performance metallic foams have emerged as a range of materials with great potential due to its excellent strength-density ratio. In the transportation industries, such as automotive or aeronautic, high energy absorption capacity combined with low density are interesting properties for use in stiffness related parts and passive safety structures (Banhart, 2001).

Due to its low density, high strength and excellent energy absorption in compression, the use of metal foams in impact-related parts has been increasingly considered in order to increase the passive safety. The mechanical behavior of metal foams depends on the structure of cells, density and properties of the base material they are made. The efficiency obtained in the use of metallic foams in structural applications requires a detailed characterization of its deformation behavior for different loads and different geometries. The size and shape of the cells or pores determines their properties, namely their behavior depends on how the solid is distributed in the porous structure (Olurin et al., 2000).

Although the relative density is the most dominant factor in determining the behavior and strength of a metal foam, other parameters such as distribution and configuration of the cells can also have great influence on the mechanical behavior. Kou and co-authors (Kou et al., 2008) proposed two types of open-cell foam structures using uniform and dual-size base cell configurations (Fig. 1). Uniform cell metal foams have a spherical shape and are closely compact. It is assumed that the cellular structure has a face-centered cubic arrangement. Dual-size foams have fillers forming a secondary link that is disposed in voids existing in uniform foam (Fig. 1). The distance between two adjacent centers of large fillers is a , the radius of large fillers and secondary fillers are R and r , respectively.

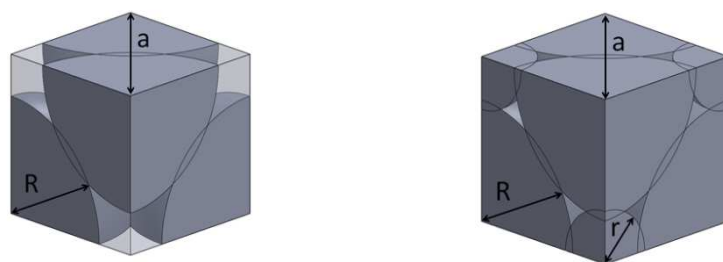


Fig. 1. Compacted structures of fillers in open-cell arrangements, left: uniform-size structure; right: dual-size structure (Kou et al., 2008)

In this work, experimental results on the compression behavior of uniform and dual-size metal foams are presented and discussed. The structures were manufactured by lost-wax casting using 3D printed components for structure definition (Fig. 2). Compression tests were performed on test samples. Results for stiffness and energy absorption were obtained and compared on weight efficiency basis.

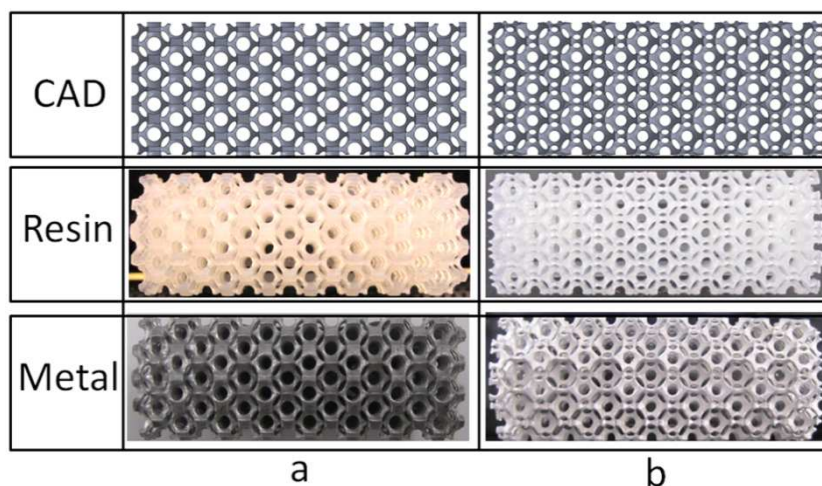


Fig. 2. CAD, resin and metal specimens obtained: US cellular structure (a) and DS cellular structure (b)

MATERIALS AND EXPERIMENTAL METHODS

In this study, a commercial AlSi12 alloy (A413.1) was used for the manufacturing of cellular structures. This alloy was selected based on previous experience in manufacturing structures with very thin walls. The composition of the alloy is presented in Table 1

Table 1. Nominal chemical composition of A413.1 aluminium alloy (wt.%)

	Si	Cu	Fe	Mg	Mn	Zn	Ni	Al
Wt. [%]	11,0-13,0	1,0	1,0	0,10	0,35	0,40	0,50	balance

For the manufacturing process a preliminary 3D prototyping stage is used. The resin used in the rapid prototype (RP) machine was a photosensitive resin, DC 500 [DWS S.r.l., Zané, Italy], that is specifically designed to allow the production of high-definition, detailed parts and smooth surfaces. A commercial gypsum [Ranson& Randolph, Ultra-Vest, Maumee,OH, USA] was used in the lost wax casting as investing material.

Based on previous research work (Kou et al., 2008) idealized structures of open-cell metallic foams were designed using CAD software (SolidWorks). Cylindrical models with 40mm height and 16mm diameter were selected for the quasi-static compression tests. Two types of

structures were studied: one based on a single spherical open-cell with 2 mm radius (R) repeated in X, Y e Z directions, closely compacted, with fcc-like arrangement – Uniform-Size (US); and other based on two sized spherical open-cells, with 2 mm (R) and 0,85mm (r) radius ($r=0.425.R$) and organized like the Uniform Size– Dual-Size (DS) (Fig. 1).

The obtained models in CAD software were exported to a stereolithography (STL) machine (Digital Wax 008, DWSS.r.l., Zané, Italy). Eight resin samples were prototyped: four with uniform-size (US) cellular structure; and four with dual-size (DS) cellular structure. After each prototyping cycle, the resin models were cured for 30 minutes in an ultraviolet curing unit (Digital Wax Model S, DWS S.r.l., Zané, Italy) to final solidification.

The investment flask was prepared following the manufacturer instructions (Ranson& Randolph, Ultra-Vest, Maumee, OH, USA). The metallic specimens were obtained by lost wax casting using a vacuum/pressure casting machine (Indutherm VC 400, Walzbachtal/Wössingen, Germany). The AlSi alloy was melt in a graphite crucible at 635°C on the top chamber under argon atmosphere ($p_1 = p_{atm}$) while the flask was placed in the bottom chamber under vacuum ($p_2=0,1\text{mbar}$) at 350°C. After the alloy's melting, an over pressure of 0.75bar (p_3) was added to the top chamber followed by the pouring of the metal at 635°C ($p_4=0,1\text{mbar}$) (Fig. 5.b) into the mold cavity. After casting, when the mold reached 500°C, it was inserted into a water container at room temperature that caused the disintegration of the investment. The residual investment in the metal tree was removed in an ultrasonic water cleaner for 10 minutes.

In order to analyze mechanical properties the specimens were submitted to uniaxial compressive tests (Fig. 3). The displacement rate was 10 mm/min and the tests stopped when the displacement reached 26mm. Tests were performed in a universal testing machine (Instron 8874, MA, USA) at room temperature and ambient air. From the load-displacement acquired data, the maximum initial load ($P_{m\acute{a}x}$), stiffness (S_f) and the absorbed energy at 5 and 15 mm of displacement (E_5 and E_{15} , respectively), were obtained.

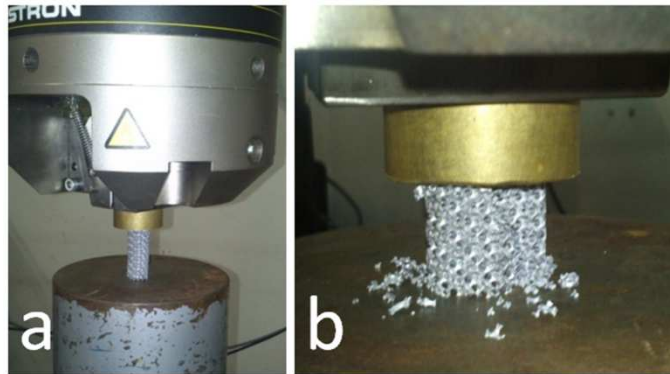


Fig.3. Compressive tests: (a) initial stage; (b) final stage.

RESULTS

Compression tests results are presented in Fig. 4 for all metallic specimens of Uniform-Size (Fig. 4.A) and Dual-Size structures (Fig.4.B). From these results it was possible to extract: the maximum initial load ($P_{m\acute{a}x}$) in the first inflection point of the loading curve; the stiffness (S_f), by the slope of the curve in elastic regime; and the absorbed energy at 5 and 15 mm of displacement obtained by calculating the area below the curve. These values and their specific values (per gram) are presented in table 2.

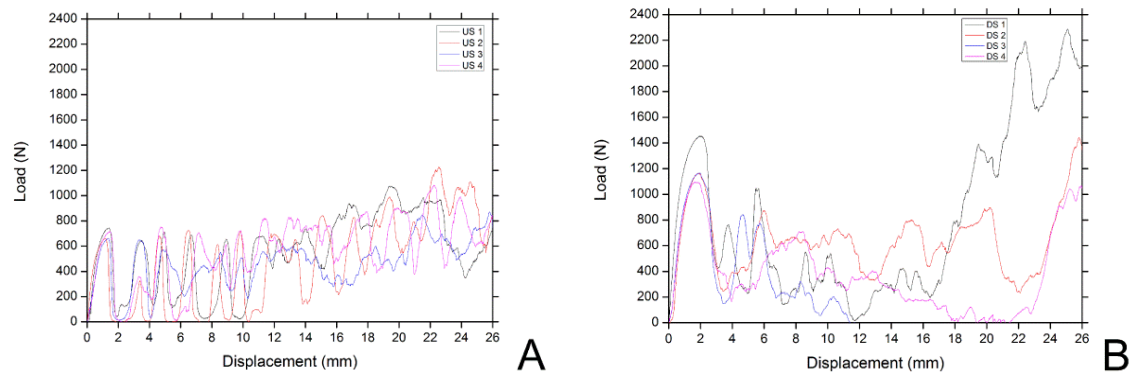


Fig.4.Compression tests results– Uniform-Size Structure (A); Dual-Size Structure (B).

Table 2. Results for mechanical behavior in the compression tests

Specimen	Mass (g)	P_{max} (N)	Specific P_{max} (N/g)	Stiffness (N/m)	Specific Stiffness (N/m.g)	Energy 5 (J)	Specific Energy 5 (J/g)	Energy 15 (J)	Specific Energy 15 (J/g)
US 1	3,23	744,9	230,6	10,7E+05	3,31E+05	1,97	0,61	5,94	1,84
US 2	3,27	662,3	202,5	8,99E+05	2,75E+05	1,22	0,37	4,32	1,32
US 3	3,02	660,4	218,7	7,20E+05	2,38E+05	1,65	0,55	7,07	2,34
US 4	3,07	716,1	233,2	9,43E+05	3,07E+05	1,67	0,54	6,05	1,97
Average	3,15	695,9	221,3	9,09E+05	2,88E+05	1,63	0,52	5,85	1,87
Standard deviation	0,12	41,6	14,0	1,46E+05	0,40E+05	0,31	0,10	1,14	0,42
DS 1	3,32	1454,9	438,2	16,8E+05	5,06E+05	4,09	1,23	7,45	2,24
DS 2	2,83	1165,8	411,9	8,71E+05	3,08E+05	3,07	1,08	9,10	3,22
DS 3	2,91	1165,2	400,4	9,93E+05	3,41E+05	3,26	1,12	4,96	1,70
DS 4	3,00	1097,5	365,8	9,89E+05	3,30E+05	2,86	0,95	6,96	2,32
Average	3,02	1220,9	404,1	11,3E+05	3,71E+05	3,32	1,10	7,12	2,37
Standard deviation	0,21	159,3	30,0	3,71E+05	0,91E+05	0,54	0,12	1,70	0,63
Variation		+75.4%	+82.6%	+24.3%	+28.8%	+103.7%	+111.5%	+21.7%	+26.7%

As shown in Fig.4, the compressive behavior of Uniform Size structure is similar to the Dual Size until the first layer collapses. At this stage Dual Size structure withstood a significantly higher initial load. From this stage, as the structure densification is unique for each sample, the compressive behavior is also different. This densification behavior is largely related to the extensive fracture that occurs within the sample’s geometry.

Results show that the specific P_{max} (N/g) withstood by Uniform Size (US) structure was approximately 212 N/g whereas that withstood by the Dual Size (DS) structure was approximately 404 N/g, i.e. the strength exhibited by the Dual Size structure was ~83% higher than that of the Uniform Size.

In what concerns specific stiffness, the dual size structure obtained an average value 29% higher than the uniform size structure. These values are consistent with values from numerical simulation presented in paper proposing the dual size structure (Kou et al., 2008).

Regarding specific absorbed energy registered until 5 mm of displacement, the dual size structure displayed an average absorbed energy significantly higher than the uniform size structure – around 112%. However, for a higher displacement (15 mm) the specific absorbed energy of the dual size structure was approximately 27% higher than that of the uniform size structure. This is attributed to the much higher initial load peak that contributes to the energy calculation in the first 5 mm of displacement.

Based on the experimental data, one can conclude that the Dual Size structure exhibited general enhanced mechanical behavior over the Uniform Size structure. These improvements showed to be highlighted in the maximum initial load supported (+83%) and in the absorbed energy until 5 mm of displacement (+112%). However, more realistic values of stiffness (29%) and energy absorption at 15 mm (27%) are to be considered for a validation of the modified geometry for mechanical applications. This analysis is based on the greater contribution of the maximum load and associated energy absorbed in the initial phase of collapse behavior.

CONCLUSIONS

In this research work two types of metal foams were manufactured and analyzed, having different cell structures: uniform cell structure and dual-size cell arrangement. The structures were manufactured by lost-wax casting using 3D printed components for internal structure definition. Results for stiffness and energy absorption were obtained and compared on weight efficiency basis.

The compression tests showed that the specific $P_{\text{m\acute{a}x}}$ (N/g) withstood by the Dual-Size(DS) structure was approximately ~83% higher than that of the Uniform Size, while stiffness had an improvement of 29%. Specific absorbed energy registered for 5 mm of displacement presented a significant improvement (around 112%). For a higher displacement (15 mm) the specific absorbed energy of the dual size structure was approximately 27% higher than that of the uniform size structure. These results are indicative of a higher efficiency of the dual-size structures that may be therefore considered for use in components subjected to impact or compression loading, both in stiffness and crash-energy absorption requirements.

ACKNOWLEDGMENTS

The authors are grateful to the Portuguese Foundation for Science and Technology (FCT) who financially supported this work, through the project PTDC/EME-PME/115668/2009.

REFERENCES

- Banhart J., *Manufacture, characterisation and application of cellular metals and metal foams*, Progress in Materials Science, Volume 46, Issue 6, Pages 559–632, 2001.
- Kou D., Li J., Yua J, Cheng H., *Mechanical behavior of open-cell metallic foams with dual-size cellular structure*, Scripta Materialia, 59, pp. 483–486, 2008.
- Olurin O., Fleck N., Ashby M., *Deformation and fracture of aluminium foams*, Materials Science and Engineering, A291 (2000), 136–146, 2000.